Hindawi
Mathematical Problems in Engineering
Volume 2023, Article ID 7742125, 15 pages
https://doi.org/10.1155/2023/7742125

Research Article

Research on the Theory and Numerical Simulation of Mine Pressure Behavior in Steeply Inclined Thick Coal Seams

Yuxi Huang[1] **and Xiaoyang Cheng**[2,3,4]

[1]*School of Mining, Liaoning Technical University, Fuxin 123000, China*
[2]*China Coal Research Institute, Beijing 100013, China*
[3]*State Key Laboratory of the Gas Disaster Detecting, Preventing and Emergency Controlling, Chongqing 400037, China*
[4]*China Coal Technology and Engineering Group Chongqing Research Institute, Chongqing 400037, China*

Correspondence should be addressed to Yuxi Huang; huangyuxi1900@126.com

Received 18 October 2022; Revised 24 November 2022; Accepted 15 April 2023; Published 26 May 2023

Academic Editor: Fuqiang Ren

This paper aims to study the law of pressure behavior and the characteristics of mutual influence in the process of steeply inclined coal seam mining. Based on the geological and engineering conditions of the B8 coal seam in Nanshan coal mine, this paper explores the law of mine pressure behavior in the process of steeply inclined coal seam mining by means of theoretical analysis and FLAC3D numerical simulation. Based on this, this paper also examines the influence of the interaction range between coal seams, the reasonable setting size of the section coal pillar, and the mining distance of the working face on the return air roadway. The results suggest as follows: (1) With an increase in the coal seam dip angle, the difference in the abutment pressure plastic zone between upper and lower coal pillars increases, and when mining in steeply inclined coal seams, the stress concentration in the lower and upper part of the working face deviates to the roof and floor respectively, which is obviously different from that of gently inclined coal seams. (2) The vertical stress above the section coal pillar changes in three stages with an increase in the width of the coal pillar, and the width of the coal pillar in the second stage can be taken as the reasonable size of the width of the coal pillar. The numerical simulation results are consistent with the theoretical calculation results, which indicate the high reliability of this method in determining the reasonable coal pillar size. (3) With an increase in the mining distance in steeply inclined coal seams, the maximum pressure around the working face and above the return air roadway has gone through three stages. When the distance between the working face and the adjacent return air roadway is close, the pressure above the return air roadway increases sharply, and disturbance is stronger.

1. Introduction

As the primary energy of consumption, coal plays a critical role in China's energy structure and national economy. With a decrease in high-quality coal resources in China, the mining activities of large dip coal seams are gradually increasing [1]. The steeply inclined coal seam generally refers to the coal seam with a buried dip angle of 35°~55° [2] and is universally considered to be the most difficult coal seam to mine in the mining field [3]. The mine pressure behavior caused by mining in steeply inclined coal seams is obviously different from that in gently inclined coal seams. Therefore, it is of great significance to develop a reasonable mining plan to accurately grasp the mine pressure behavior in the mining process of steeply inclined coal seams. For this reason, many scholars have studied the mine pressure behavior and the disturbance in the process of mining of steeply inclined seams from different angles.

Liu et al. [4] pointed out that, in steeply inclined coal seams, the stress exerted by the surrounding rock on the roof can be divided into the normal stress perpendicular to the rock stratum and the shear stress parallel to the rock stratum, and the shear stress is greater than the normal stress. Due to the large inclination angle, the direct roof of the upper part of the working face tends to collapse on the goaf and backfill its lower space, thus forming the support to the lower roof

[5–7] when the upper roof is suspended. Therefore, the overlying strata are subjected to asymmetric stress in tendency, resulting in asymmetric separation and caving, which brings difficulties to the management of surrounding rock. Qi et al. [8] studied the deformation and failure characteristics of surrounding rock, aiming at the phenomenon of misalignment and large deformation and failure that often occur after excavation and support of roadway in steep coal seams. Based on the small-deflection theory for elastic thin plates, Tu et al. [9] established a working face mechanical analysis model for the first time before roof fracture after coal seam mining with a large dip angle. Yang and Liu [10] used the natural arch theory to analyze the cave-in mechanism of horizontal coal roadway in steep coal seams and studied the stress distribution characteristics and failure law of surrounding rock of fully mechanized mining roadway in steep coal seams. Hong-Sheng et al. [11] pointed out that the stability of the lower roof of the working face is higher than that of the upper roof in the mining of high dip coal seams. With a gradual increase in the dip angle, the ability of rock mass to withstand slip-induced instability increases, but the ability to withstand deformation-induced instability decreases. Wu et al. [12] studied the mechanical properties and microstructure of cemented rockfill reinforced by carbon nanotubes and fractal aggregates through macroscopic mechanical and microscopic scanning tests, which can provide certain support for surrounding rock support when mining coal seams with a large dip angle. Through the above analysis, this paper reveals the disturbance influence on the confining pressure in the mining process of the steeply inclined coal seam, which provides a certain theoretical basis for on-site construction.

Based on FLAC3D numerical simulation software, Xue et al. [13] studied the variation characteristics of surrounding rock stress and energy in the mining process of the steeply inclined coal face. The results show that the working face is in a high stress state affected by the leading abutment pressure, the energy accumulation area of the roof is located in the lower end and the middle and upper part of the working face, and the energy accumulation area of the floor is located in the lower end of the working face. Lu et al. [14] studied the characteristics of pressure behavior in the process of shallow steeply inclined coal seam mining through two-dimensional numerical simulation. The results show that the law of pressure behavior in the mining process of the steeply inclined coal seam is obviously different from that of the gently inclined coal seam and the uneven settlement of the steeply inclined coal seam floor is more serious than that of the coal seam roof. Zhang and Shi [15] carried out the numerical simulation of combined mining of a large dip angle and a short-distance coal seam by a finite element method. By discussing the deformation and failure characteristics of surrounding rock, they revealed the scientific nature of combined mining of steeply inclined close coal seams. Zhang et al. [16] studied the stress redistribution and coal seam deformation characteristics under the goaf of a high-dip coal seam by using 3DEC software. The results show that, in the process of upper slicing mining, more than 75% of the coal in lower slicing is located in the effective pressure relief area. Wu et al. [17] analyzed the influence of the mining process of steeply inclined coal seams on coal seam roadway through the numerical simulation and pointed out that the difference in the rock structure on both sides of steeply inclined coal seam roadway is the root cause of roadway asymmetric failure. Qi et al. [8] studied the failure mechanism and control technology of roadway surrounding rock in deep steeply inclined coal seams under the influence of a weak structural plane by the FLAC3D numerical simulation and explored the reasonable support scheme of roadway according to the results of the numerical simulation.

The above analysis suggests that the disturbance and pressure behavior of steeply inclined coal seam mining have their own characteristics. Moreover, theoretical analysis and numerical simulation methods play a significant role in revealing the disturbance mechanism in the process of steeply inclined coal seam mining. However, at present, the law of pressure behavior and disturbance characteristics in the process of steeply inclined coal seam mining is rarely studied. In particular, there are few studies on the interaction between coal seams and the effect of coal seam mining on section coal pillars in steeply inclined coal seam mining. In the process of coal seam mining, the law of mining pressure manifestation in different regions is different. How to systematically study the characteristics of mining pressure manifestation in different regions in the process of large dip coal seam mining is the key research content of this paper, which is also the important innovation of this paper. Based on this, the paper explores the law of pressure behavior in the process of mining steeply inclined thick coal seams by focusing on the interaction between coal seams and the reasonable width of the coal pillar in steeply inclined coal seam mining and the relationship between face mining distance and roadway mining, which is expected to provide a theoretical basis and reference value for the development of on-site engineering.

2. Theoretical Analysis on the Law of Mine Pressure Behavior in Working Face

Coal and rock mass are not manually disturbed before coal mining, and the stress is in a state of equilibrium. At this point, the measured rock mass stress is the original rock stress. After coal mining, the mining stress field is formed, and the vertical pressure acting on coal seam, rock strata, and gangue within the range of surrounding rock stress redistribution is called abutment pressure. The accurate calculation of the distribution law and the range of the abutment pressure in stope have a significant application value for the adoption of reasonable support modes and methods for stope, the determination of reasonable excavation location and time of adjacent roadway, and the prevention of accidents related to the abutment pressure.

2.1. Distribution Law of Inclined Abutment Pressure in Working Face. There is a pressure peak in the abutment pressure distribution range, and the abutment pressure

distribution is divided into the plastic zone and elastic zone according to the pressure peak. The structural mechanic model is established, as shown in Figure 1.

According to the mechanical model of the inclined supporting pressure structure shown in Figure 1, the range of the plastic zone of the inclined abutment pressure in the working face is established:

$$\begin{cases} x_{\text{上侧}} = \dfrac{M\beta}{2\tan\varphi_0}\ln\left[\dfrac{\beta\left(\sigma_{y1}\cos\alpha\tan\varphi_0 + 2c_0 - M\gamma_0\sin\alpha\right)}{\beta\left(2c_0 - M\gamma_0\sin\alpha\right) + 2P_x\tan\varphi_0}\right], \\ x_{\text{下侧}} = \dfrac{M\beta}{2\tan\varphi_0}\ln\left[\dfrac{\beta\left(\sigma_{y1}\cos\alpha\tan\varphi_0 + 2c_0 + M\gamma_0\sin\alpha\right)}{\beta\left(2c_0 + M\gamma_0\sin\alpha\right) + 2P_x\tan\varphi_0}\right], \end{cases} \tag{1}$$

where $x_{\text{upperside}}$ refers to the range of the plastic zone of the inclined abutment pressure on the upper side of the stope, M refers to the thickness of the mining coal seam, β refers to the lateral pressure coefficient of the face where the ultimate strength is located, φ_0 refers to the friction angle at the interface between the coal seam and the roof and the floor, σ_{y1} refers to the peak value of the abutment pressure, α refers to the dip angle of the coal seam, c_0 refers to the cohesion at the interface between the coal seam and the roof and the floor, γ_0 refers to the average volume force of coal, and P_x refers to the binding force of roadway support on the coal wall along the x direction.

The upper side of the stope means that the coal pillar of the goaf is located on the upper side of the upwind roadway, and the lower side of the stope means that the coal pillar of the goaf is located on the lower side of the conveyor roadway. It can be observed from formula (1) that the range of the plastic zone of the inclined abutment pressure correlated with the dip angle of the coal seam. Such a correlation is not noticeable when the dip angle of the coal seam is small, but with an increase in the dip angle of the coal seam, the difference in the plastic zone of the abutment pressure between the upper side and the lower side of the coal pillar increases.

In the subsequent analysis of the mining pressure of the working face, coal pillars in sections, and the interaction between coal seams, the stress values at different positions were calculated according to the abutment pressure model shown in Figures 1 and 2. At the same time, the yield condition and the plastic zone range of coal and rock are judged according to the corresponding criterion.

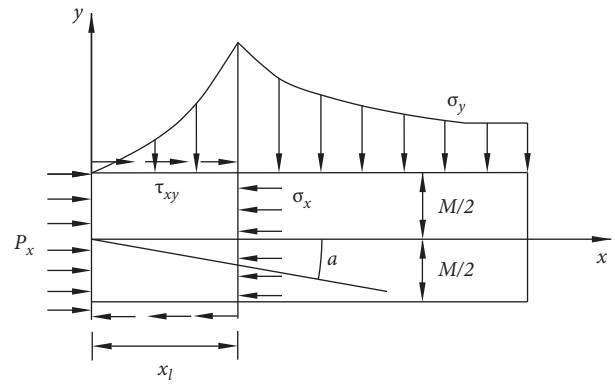

Figure 1: Mechanical model diagram of inclined abutment pressure structure [18].

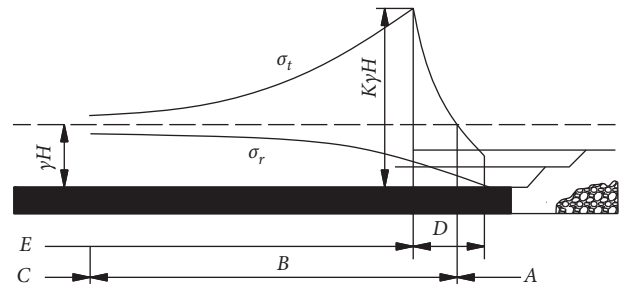

Figure 2: Distribution of strike abutment pressure in the mining face: (a) stress reduction area; (b) stress increase area; (c) original rock stress area; (d) limit equilibrium zone; (e) elastic zone [19].

2.2. Distribution Law of Strike Abutment Pressure in Working Face. The movement and stress redistribution of the strata around the stope caused by coal seam mining have a great impact on the deformation and failure of the surrounding rock of the steeply inclined coal seam. When backstopping in the working face, the strata in the irregular caving zone are in a loose state and the overlying strata are largely in a suspended state, which makes it necessary to transfer the weight of the suspended strata to the coal body in front of the working face. At this point, the goaf is a lower area than the original rock stress, and the abutment pressure of the coal in front of the working face is much higher than that of the original rock, as shown in Figure 2.

The range of the plastic zone of strike support pressure in the working face is established according to the mechanical model of the strike support pressure structure shown in Figure 2:

$$x_0 = \frac{M}{2fk_p}\ln\left[\frac{K\gamma H\cos\alpha + \left(2Ck_p + M_0S_t/2fk_p\right) - \left(M_0S_t/2fk_p\right)e^{\left(2fk_p/M_0S_t\right)\left(\sigma_c - \sigma_c^*\right)}}{k_p p_x + \sigma_c^* + (/)}\right]. \tag{2}$$

In the formula, M refers to the coal seam mining thickness, f refers to the friction coefficient between the coal seam and the roof and floor, $f = \text{tg}\varphi$ (φ refers to the internal friction angle at the coal-rock contact), K refers to the stress concentration factor, H refers to the buried depth of the coal seam, α refers to the coal seam dip angle, γ refers to the bulk

density of the overlying strata, C refers to the cohesion of the coal layer, M_0 refers to the softening modulus of the coal, S_t refers to the strain gradient of the coal in the plastic zone, p_x refers to the protective force of the supporting plate of the working face to the coal wall, σ_c refers to the uniaxial compressive strength of coal, and k_p refers to the internal friction angle of coal.

3. Analysis and Discussion of Numerical Simulation Results

3.1. Introduction of the Project and the Establishment of the Model. Taking the B8 coal seam of Xiaogou coal mine in Nanshan coal mine in Shihezi city in China as the research object, this paper examines the law of pressure behavior of the steeply inclined coal seam. The dip angle of the B8 coal seam is 38°~42°, the thickness of the coal seam is 4.2 m, the old roof is 14.6 m fine sandstone, the direct roof is 20.2 m siltstone, and the direct bottom is 1.2 m fine sandstone. In this paper, through field sampling, the corresponding physical and mechanical properties of rock are measured by using indoor rock mechanic testing machine, and then, the corresponding model is established by using FLAC3D numerical simulation software. In FLAC3D numerical simulation software, the abutment pressure distribution model in Figures 1 and 2 is used to study the pressure behavior law of a high-dip coal seam. The Mohr–Coulomb plastic constitutive relation and the yield criterion are adopted in the numerical simulation process, and the plastic flow of rock mass is not considered. The discriminant expression is

$$f_s = \sigma_1 - A\sigma_3 + 2B\sqrt{N_\varphi}, \tag{3}$$

where σ_1 and $\sigma_3$are the maximum and minimum principal stresses, respectively, B and φ are cohesion and the internal friction angle, respectively, and $N_\varphi = (1 + \sin\varphi)/(1 + \sin\varphi)$. When $f_s \geq 0$, the material is in a plastic flow state. When $f_s < 0$, the material is in the elastic deformation stage. The values of physical and mechanical parameters in the simulation process are shown in Table 1.

3.2. Research on the Law of Mine Pressure Behavior in Mining Face. According to the theoretical model shown in Figure 2, the rock pressure behavior law of the mining face is studied by using the FLAC3D numerical simulation software, as shown in Figure 3.

After extracting the specific values from the numerical simulation results, the vertical stress variation curves at different positions of the mining face are obtained, as shown in Figure 4.

As can be observed in Figures 3 and 4, after mining, the stress concentration in the lower part of the working face deviates to the roof, the stress concentration in the upper face deviates to the floor, the influence range of stress in the lower part of the working face is 20 m, and the stress concentration appears in the position of about 3 m. These characteristics are obviously different from those of the gently inclined coal seam. The area within 0–3 m from the lower part of the working face is the stress reduction area, the area within 3–20 m is the stress increase area, and the area beyond 20 m from the lower part of the working face is the stress stable area. In the process of mining large dip coal seams, the maximum stress is about 18 MPa and the location is about 5 m from the lower part of the working face.

3.3. Research on the Pressure Behavior of the Coal Pillar in the Coal Seam with a Steeply Inclined Angle

3.3.1. Research on the Stress and Deformation Characteristics of the Section Coal Pillar. In order to explore the influence of the angle on the pressure behavior of the coal pillar in coal seams with a steeply incline angle, the models of a coal seam dip angle of 35°, 40°, and 45° and a section pillar of 20 m were established by using FLAC3D numerical simulation software. Based on the existing research results, verification is completed and good results are obtained. The numerical simulation results are shown in Figure 5 [20].

The results of the numerical simulation cloud map in Figure 5 suggest that the maximum concentrated stress of the coal pillar in the working face of the steeply inclined coal seam is located at the top of the coal pillar near the roof of the upper working face. In order to further quantitatively characterize the effects of different dips and distances, the results in Figure 3 are extracted, as shown in Figure 6 [20].

As can be observed in Figure 6, with an increase in the dip angle, the concentrated stress action point shifts to the upper part of the roof (the upper end of the coal pillar) and to the coal wall of the working face, and the influence range of vertical stress becomes smaller with an increase in the dip angle. When the dip angle of the working face is 45°, the saddle-shaped stress distribution curve appears in the coal pillar, indicating that the stress in the working face and the lateral stress of the coal pillar are no longer superimposed.

3.3.2. Research on Stress and Deformation Characteristics of the Coal Pillar with Different Width. In order to study the law of deformation and failure of the coal pillar in different width sections under a large dip angle, numerical models with a coal pillar width of 5 m, 10 m, 15 m, 20 m, 25 m, and 30 m are established, respectively, for numerical simulation analysis under the condition that the dip angle of the coal seam is 40 and that the range of the goaf is constant, as shown in Figure 7 [20].

In order to better reflect the law in Figure 7, the variation results of vertical stress under the coal pillar with different widths with roadway distance are extracted, as shown in Figure 8 [20].

As shown in Figures 7 and 8, the upper side of the coal pillar, that is, the side near the goaf, is affected by the upper goaf, resulting in stress concentration. From the vertical stress curve, it can be observed that when the width of the coal pillar is about 0~10 m, the overall bearing pressure of the coal pillar is larger, and on one side of the roadway, the stress value is obviously higher than that of other width coal pillars. When the width of the coal pillar is 5 m, the maximum stress is 14.4 MPa, and when the width of the coal pillar is 10 m, the maximum stress is 20 MPa. When the width of the coal pillar is 15~30 m, the maximum stress is

Table 1: Physical and mechanical parameters in the simulation process.

Rock stratum	Elastic modulus (GPa)	Cohesion (MPa)	Internal friction angle (°)	Tensile strength (MPa)
Old roof	48.6	5.7	36	4.2
Direct roof	52.1	2.2	32	4.0
Coal	2.9	2.0	30	0.35
Direct bottom	47.8	5.6	35	4.1

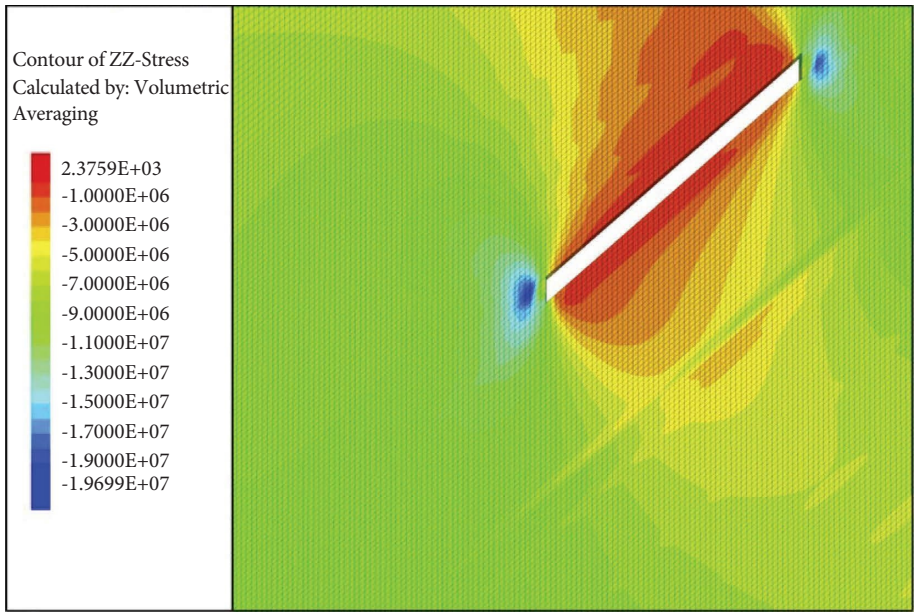

Figure 3: Cloud map of stress distribution in mining face.

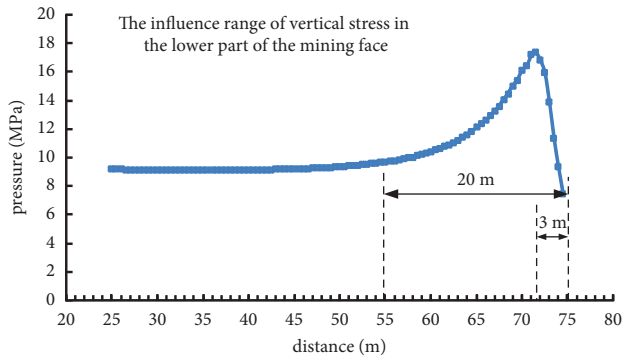

Figure 4: Stress distribution diagram at different positions of mining face.

18 MPa. Although the maximum stress when the coal pillar width is 15~30 m is greater than that when the coal pillar width is 5 m, with an increase in the coal pillar width, the maximum stress value is gradually far away from the roadway and the influence of the goaf roof on the roadway starts to decrease, thus ensuring the safe operation of the roadway. When the width of the coal pillar is more than 20 m, the "saddle-shaped" stress on the side of the coal pillar is no longer superimposed on each other. Therefore, based on the numerical simulation results and the recovery rate, the reasonable width of the roadway is set as 15 m~20 m.

3.3.3. Theoretical Study on the Reasonable Size of the Section Coal Pillar. In Section 3.3.2, the force and deformation characteristics of the coal pillar with different widths are numerically simulated, through which the reasonable width of the coal pillar is determined to be 15~20 m. In order to further verify the stability and reliability of the numerical simulation results, a theoretical study on the mine pressure behavior of the section coal pillar was carried out. The stress diagram of the section coal pillar is shown in Figure 9.

The coal strata at the upper end of the goaf area in the upper part of the working face are defined as the sliding rock mass. The force F_1 along the normal direction of the overlying strata of the sliding rock mass acts on the vertical plane of the sliding rock mass, and F_2 acts on the sliding rock mass along the bedding direction. At the same time, the sliding rock mass is also affected by its own gravity component F_4 along the normal direction, inclination component F_3, and friction on the upper and lower surfaces. The stress relationship along the dip direction when the sliding rock mass is stable is as follows:

$$F_1 f_1 + (F_1 + F_4) f_1 \geq F_2 + F_3. \tag{4}$$

In the formula, $F_1 = q_5 L_0 \cos\alpha$, L_0 refers to the width of the coal pillar, q_5 refers to the load of the overlying strata on the sliding rock mass, α refers to the dip angle of the coal seam, $F_1 = q_5 L_0 \cos\alpha$, $F_3 = \gamma_1 \Sigma h_i L_0 \sin\alpha$, γ_1 refers to the average volume force of the sliding rock mass, Σh_i refers to the total

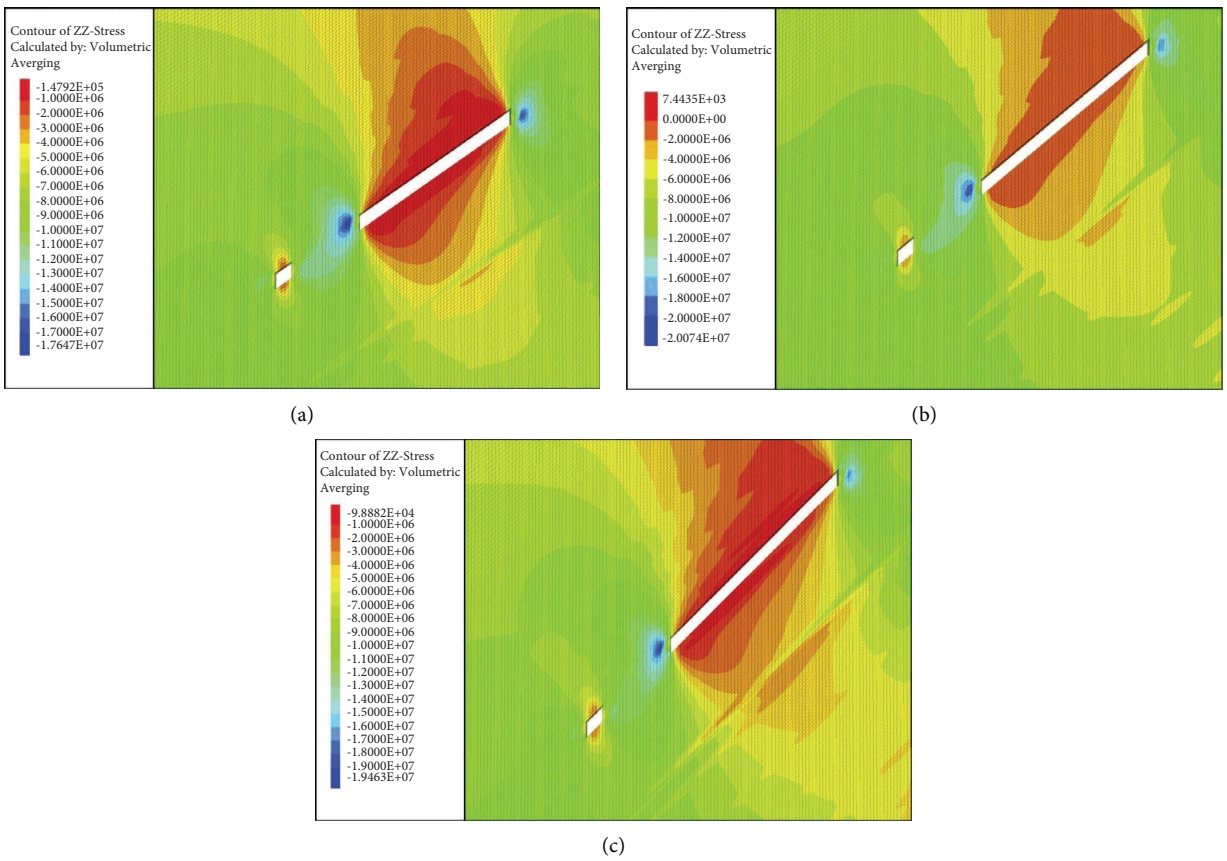

Figure 5: Cloud map of vertical stress distribution of the coal pillar at different dip angles: (a) 35°; (b) 40°; (c) 45°.

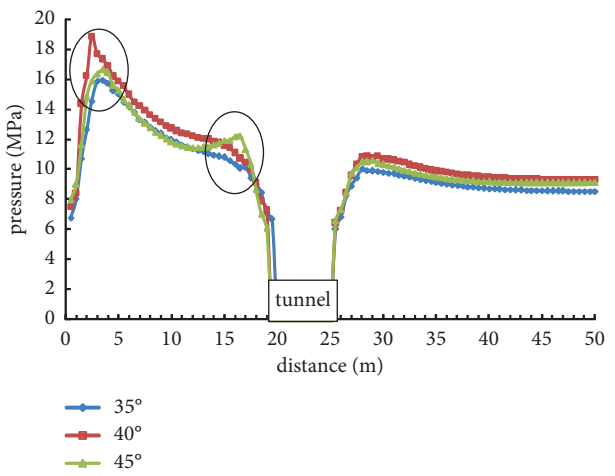

Figure 6: Stress distribution curve of the coal pillar in the coal seam with different angles.

thickness of the sliding rock mass in the upper part of the working face, $F_4 = \gamma_1 \Sigma h_i L_0 \cos\alpha$, and f_1 and f_2 refer to the friction coefficients between the upper and lower surfaces of the sliding rock mass, respectively. The following expression can be obtained by bringing the above values into formula (4):

$$q_5 \geq \frac{\sin\alpha - f_2 \cos\alpha}{(f_1 + f_2)\cos\alpha - \sin\alpha} \gamma_1 \Sigma h_i. \quad (5)$$

When the dip angle of the coal seam is greater than 45°, the right molecule of formula (5) is a real number greater than zero, and when the dip angle of the coal seam is less than 90°, the action load q_5 of the overlying strata on the sliding rock mass is a real number greater than zero. Therefore, when $(f_1 + f_2)\cos\alpha - \sin\alpha$ is negative, $q_5 \geq 0$ is always workable. Thus, it can be concluded that there is no slip and instability of the coal pillar in the section when $\alpha \leq \arctan(f_1 + f_2)$ and that there is a danger of slip when $\alpha \geq \arctan(f_1 + f_2)$.

In the above formula $h_1 = H_m + M$, M is the coal seam mining height of the working face. The particularity of the occurrence condition of the steeply inclined coal seam determines that the movement form of the overlying rock in the working face is different from that in the near-horizontal coal seam. When the hanging width of the upper strata of the working face is less than the fracture step of the overlying strata, the overlying strata stop falling, the length of the roof no longer changes, and the total thickness of the falling strata can be measured. Therefore, H_m can be determined according to the actual occurrence conditions of coal strata in the specific working face.

A balanced pressure arch structure can be formed among the upper old roof of the high inclination face, the gangue filling in the lower part of the working face, and the coal pillar in the upper section of the working face. At equilibrium, the total weight of the overlying strata is supported by

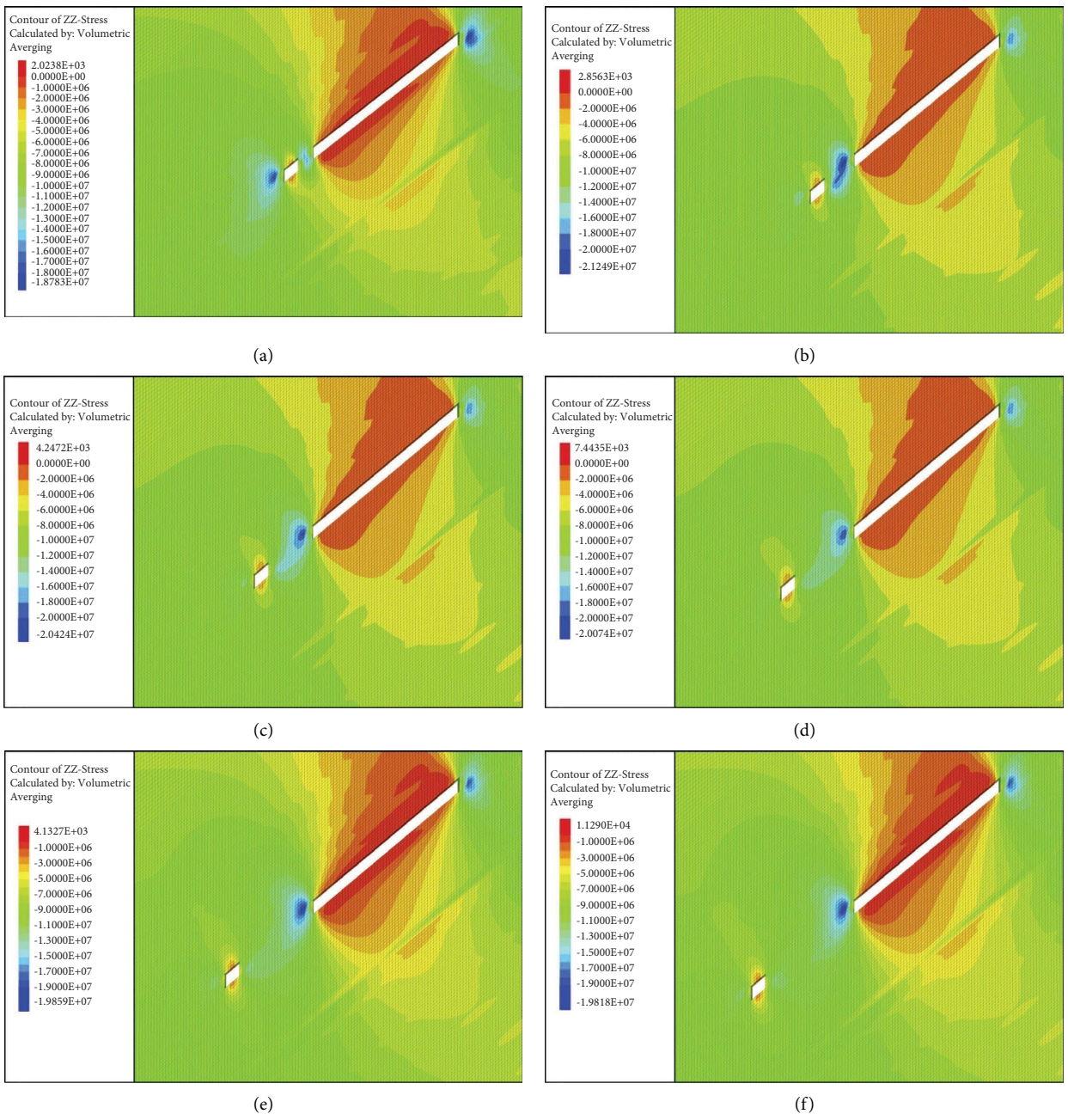

Figure 7: Cloud map of stress distribution of the coal pillar in different width sections: (a) 5 m; (b) 10 m; (c) 15 m; (d) 20 m; (e) 25 m; (f) 30 m.

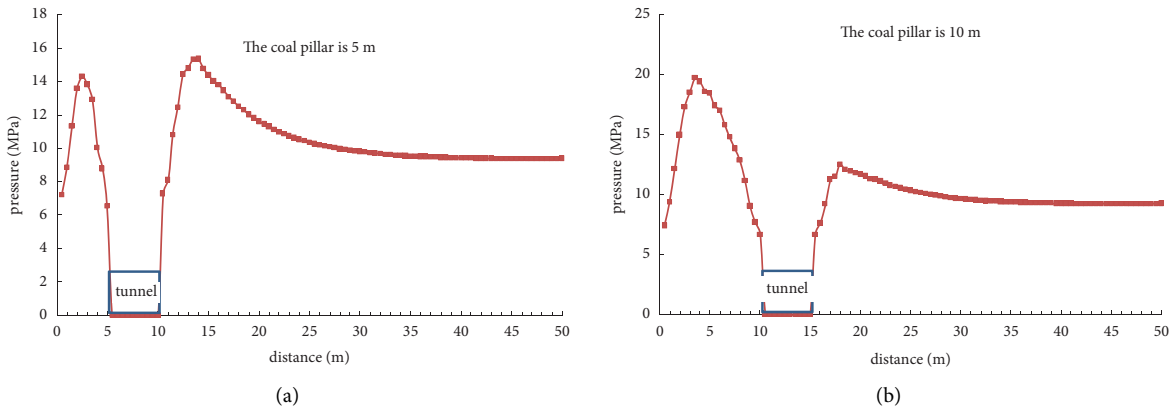

Figure 8: Continued.

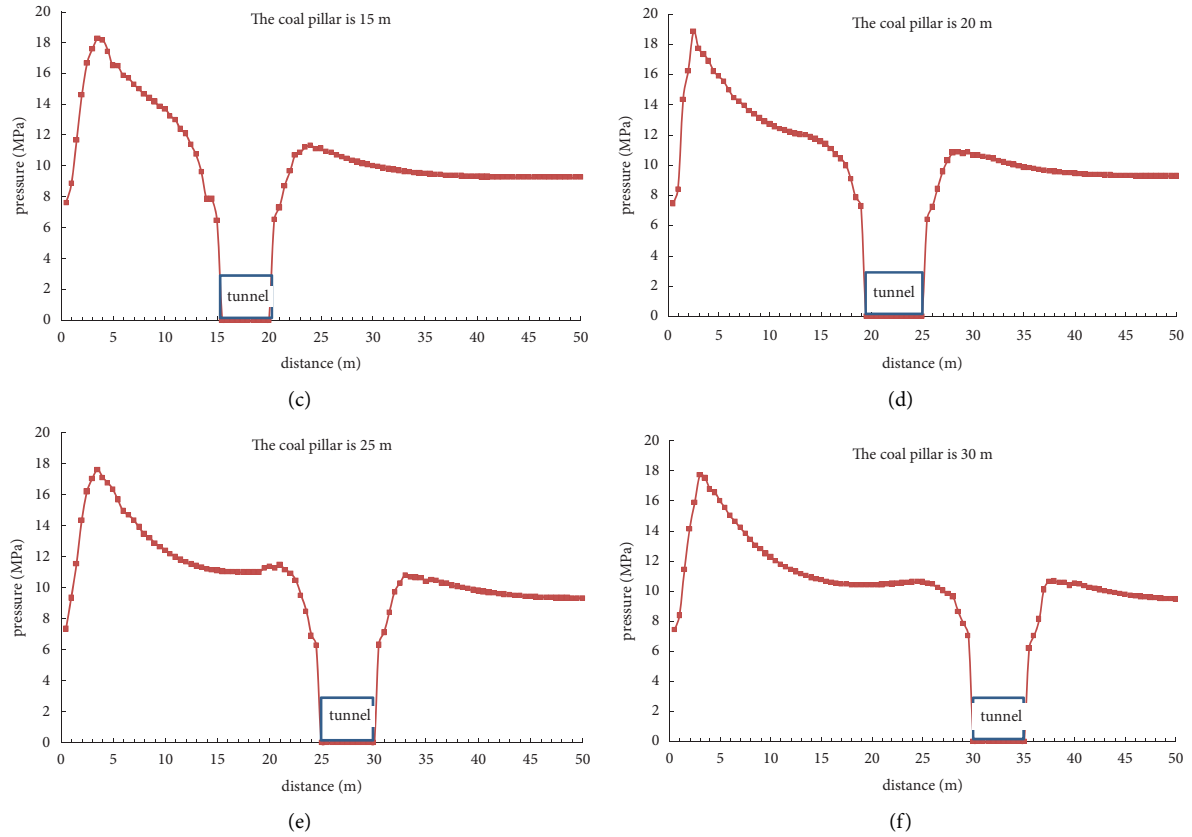

Figure 8: Vertical stress distribution curve of the coal pillar with different widths: (a) 5 m; (b) 10 m; (c) 15 m; (d) 20 m; (e) 25 m; (f) 30 m.

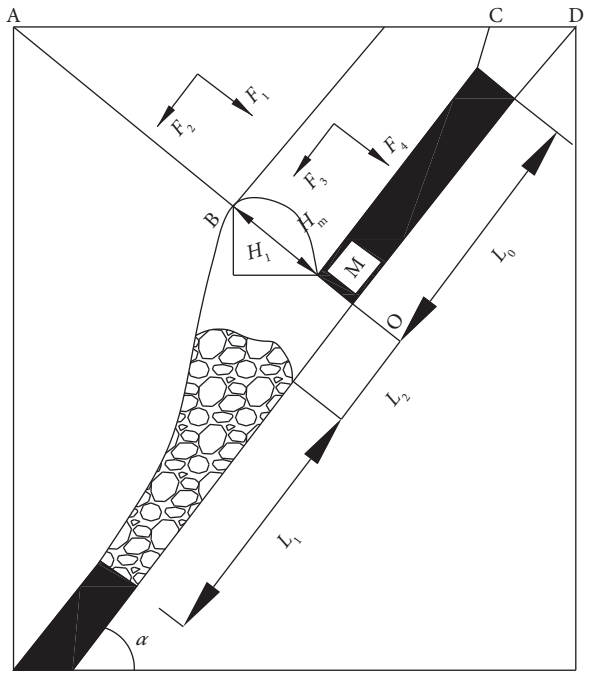

Figure 9: Stress diagram of the section coal pillar.

the section coal pillar and lower filling gangue of the working face (the support force of the bracket is negligible in comparison), as shown in Figure 10.

From the force relationship in Figure 10, it can be obtained that q_5 is

$$q_5' = \gamma H_q \frac{(L + L_0)}{L + L_0} + \frac{1}{2}\gamma \frac{(L + L_0)^2}{L_1 + L_0} \sin \alpha. \tag{6}$$

In the formula, q_5 refers to the acting force of the overlying strata on the section coal pillar. With the self-weight of the coal pillar being excluded, it can be known from the relationship between the acting force and the reaction force that the acting force of the overlying strata on the section coal pillar is equal to that of the underlying strata on the coal pillar. γ refers to the average volume force of the overlying strata, H_q refers to the buried depth at the upper end of the coal pillar, L refers to the length of the working face, and L_1 refers to the width of the filling in the lower part of the working face.

When the section coal pillar is stable, the resultant moment of each component of the section coal pillar is supposed to be balanced, and the following equation can be obtained by calculating the O point in Figure 10:

$$\frac{1}{2}F_1 L_0 + \frac{1}{2}F_4 L_0 + f_1 \Sigma h_i = F_2 \Sigma h_i + \frac{1}{2}F_3 \Sigma h_i. \tag{7}$$

Since the thickness of the coal seam is smaller than the buried depth of the working face and the total thickness of the goaf above the working face, it can be assumed that

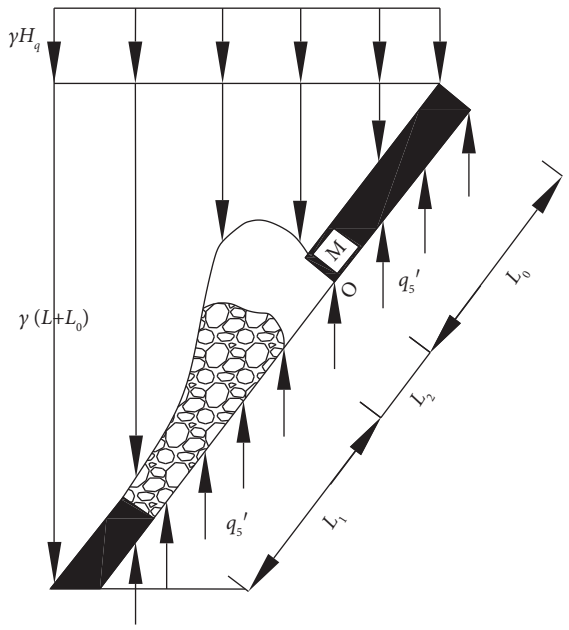

Figure 10: Stress diagram of the overlying strata.

$\gamma = \gamma_1$. By substituting $\gamma = \gamma_1$ into formula (7) and simplifying it, the following equation can be obtained:

$$q_5 = \frac{L_0 \Sigma h_i - (\Sigma h_i)^2 \tan\alpha}{2\Sigma h_i \tan\alpha + 2f_1 \tan\alpha - L_0}\gamma. \tag{8}$$

The following equation can be obtained by combining formulas (7) and (8):

$$\begin{cases} L_0 = \dfrac{P_1 + \sqrt{P_1^2 + 8\sin\alpha\tan\alpha\left((\Sigma h_i)^2 + \left(2H_q + L\sin\alpha\right)\left(f_1 + \Sigma h_i\right)\right)}}{2\sin\alpha}, \\ P_1 = 2f_1\sin\alpha\tan\alpha - 2\Sigma h_i + 2\Sigma h_i \sin\alpha\tan\alpha - 2H_q - L\sin\alpha. \end{cases} \tag{9}$$

According to formula (9), the relationship between the setting width of the section coal pillar and the dip angle of the coal seam and the mining height of the working face can be obtained. It can be seen that when the coal seam dip angle is greater than 60°, the setting size of the coal pillar in the working face is greatly affected by the dip angle, and when the coal seam dip angle is less than 60°, the setting size of the coal pillar in the working face section is less affected by the inclination angle. The reasonable setting size of the coal pillar width is linearly proportional to the mining height of the working face.

We set the height of the working face as 4.2 m, and the reasonable reserved size of the section coal pillar at different dip angles can be obtained from formula (9), as shown in Figure 11.

From Figure 11, it can be concluded that when the coal seam dip is 38°–42°, the reasonable coal pillar size is 15 m~20 m. Therefore, the theoretical calculation result of the reserved size of the coal pillar in the reasonable section of Xiaogou subore in Nanshan coal mine is 15~20 m The consistency between the theoretical calculation results and the numerical simulation results reflects the stability and reliability of the numerical simulation results.

3.4. Analysis of the Mining Influence Law of B4 Coal Seam and B8 Coal Seam. In the process of coal seam mining, the pressure behavior law above the working face is not only affected by the current abutment pressure above the working face but also related to the mining of adjacent or similar coal seams. In addition, the pressure behavior of the roadway above the working face is greatly affected by the adjacent mining face in the process of tunneling. Therefore, the study of the change law of rock pressure behavior caused by the interaction between mining not only has important theoretical significance but also has clear practical significance. This section examines the influence of similar mining coal seams on the pressure behavior in the mining process of a large inclination face by carrying out the FLAC3D

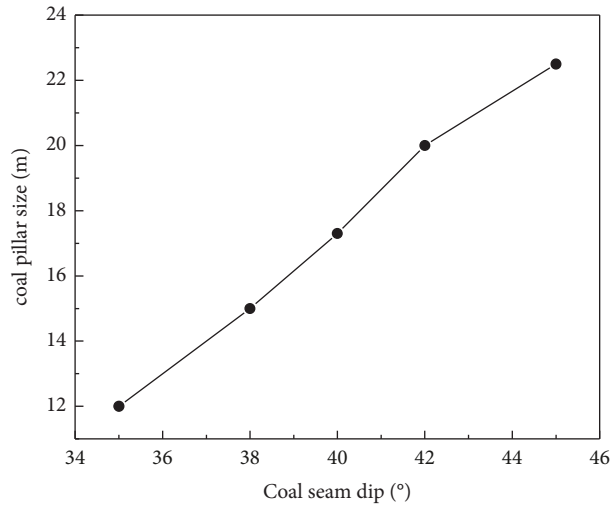

Figure 11: Variation law of reasonable coal pillar size with a dip angle of the coal seam.

numerical simulation. At the same time, the influence of the mining process of the steeply inclined working face on the ground pressure behavior above the heading roadway of the adjacent face is numerically stimulated.

3.4.1. Analysis of the Influence of B4 Coal Seam Mining on B8 Coal Seam. The thickness of the B4 coal seam is between 1.6 m and 2.26 m, the average thickness is 1.82 m, and the dip angle of the coal seam is about 40°. Most of the strata between B4 and B8 coal seams are sandstone interbeds, and the average distance between them is 66.08 m. In the process of the numerical simulation, the thickness of the B4 coal seam is 2 m and the mining length of the working face is 120 m. The model is shown in Figure 12.

According to the model established in Figure 12, the influence of B4 coal seam mining on the B8 coal seam is numerically simulated from four dimensions: plastic zone distribution, vertical displacement change, overlying strata density change, and vertical stress distribution. The results are shown in Figure 13.

The results in Figure 13 show the following:

(1) The plastic zone of B4 coal seam mining is primarily caused by shear failure and tensile failure, and the plastic zone is mainly distributed in the roof and the floor of the two cross headings. There is no plastic failure in the B8 coal seam in the middle of the B4 working face, so it is believed that the mining of the B4 coal seam does not affect the B8 coal seam.

(2) The vertical displacement primarily occurs at the upper side and roof of the upper cross heading. From the distribution of the vertical displacement of the roof, the roof deformation of the B4 coal seam does not affect the B8 coal seam, and the influence range of the B4 coal seam roof is mainly in the middle and upper parts.

(3) The change area of density primarily occurs in the position of the roof and floor, and its density does not affect the B8 coal seam from the variation range of roof density.

(4) The maximum vertical stress is in the solid coal of the two cross headings, the second is mainly distributed in the roof and floor, and the general stress distribution in the roof is larger in the middle and upper parts, which is consistent with the field ground pressure observation data of the B8 coal seam face. The simulation results show that the roof stress of the B4 coal seam has an influence on the B8 coal seam after mining, but the influence is not significant. From the numerical simulation results, when the distance between the two coal seams gradually decreases, this interaction will become increasingly significant. In addition, the maximum stress value and influence range of different coal seam spacing can be obtained from Figure 13(d). Therefore, this method can be used to judge the range of interaction of different spacing coal seams, but the precondition is to combine with specific geological conditions.

Therefore, as can be seen in Figure 13, under the assumption that the overlying strata are hard strata, after B4 coal seam mining, the plastic zone distribution, vertical displacement change, overlying strata density distribution, and vertical stress distribution do not affect or slightly affect the B8 coal seam, and the scope of influence is limited to the middle and upper parts. Although the simulation results show that the mining of the B4 coal seam has little influence on the B8 coal seam, this is mainly based on the conclusion of the actual geological conditions of Nanshan coal mine. However, the numerical simulation analysis reveals the influence range of B4 coal seam mining on the overlying coal seam, which is where the significance of this study lies.

3.4.2. Analysis of the Influence of Mining in Working Face on the Air Return Way of Adjacent Working Face. The three-dimensional numerical model is based on the layout plan of the B8 working face and the sketch drawing of +1190 m horizontal transport cross heading, and the conditions are appropriately simplified. The length of the numerical model

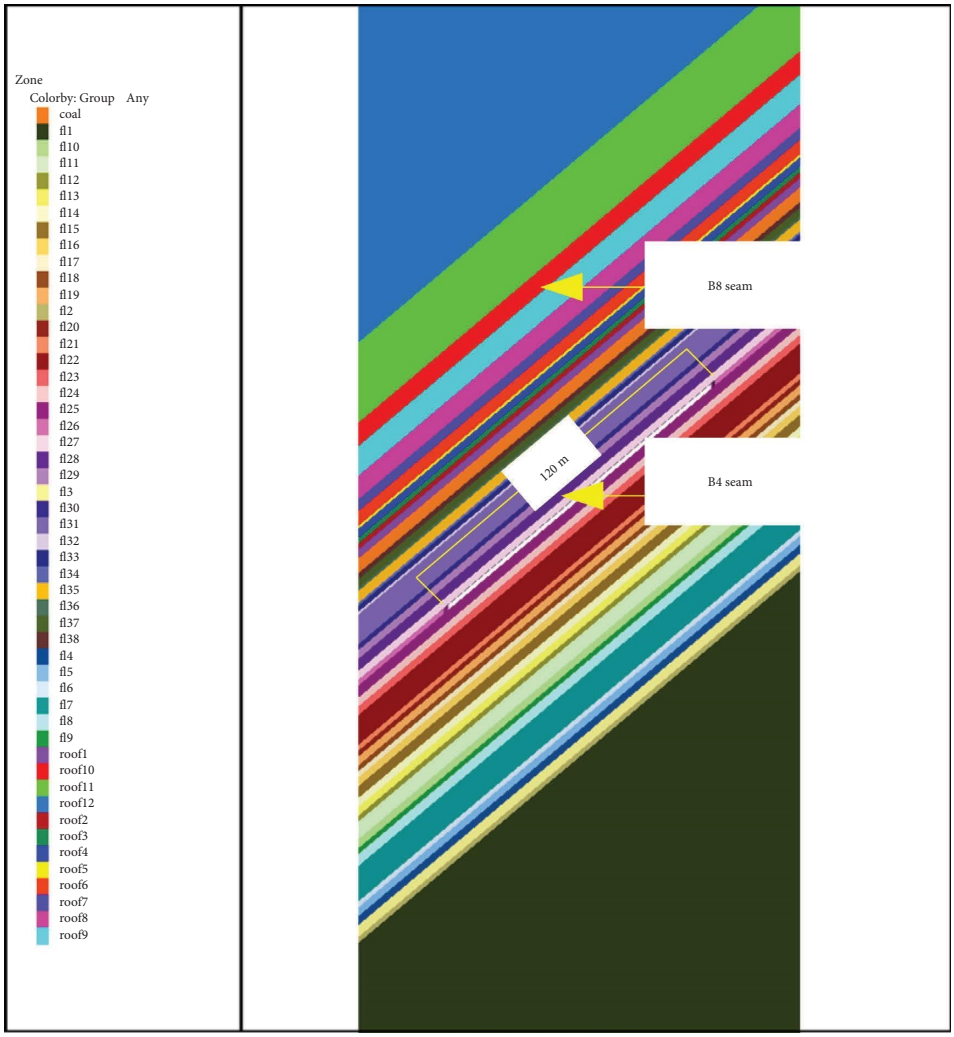

Figure 12: Simulation model diagram.

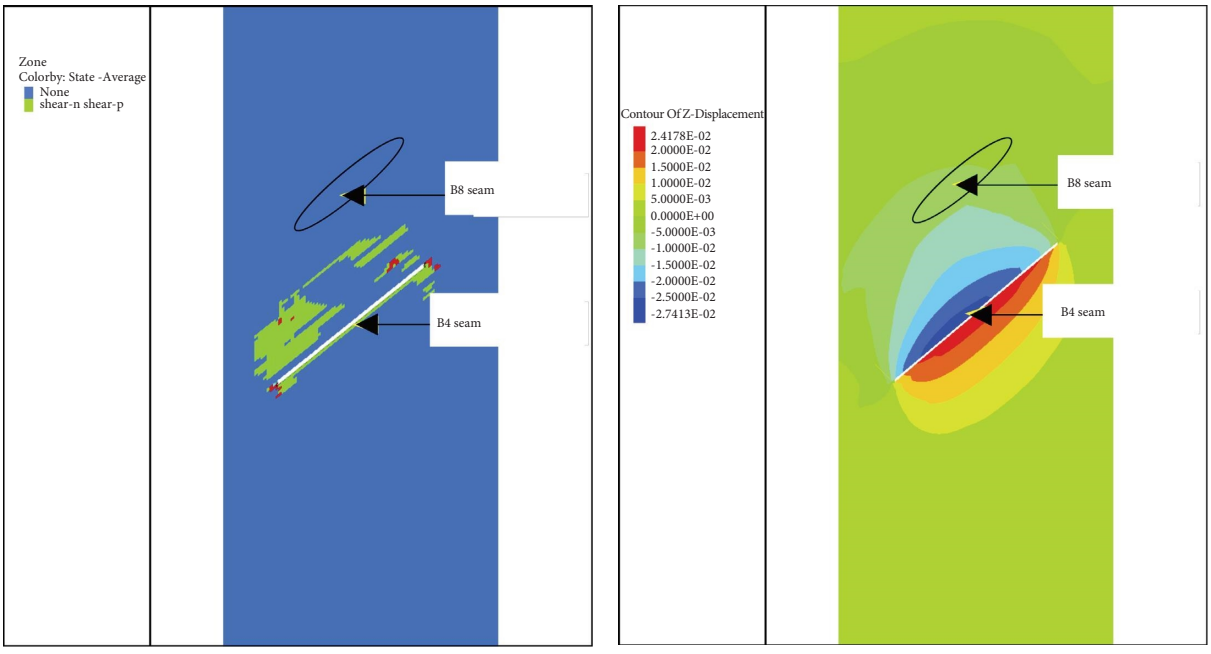

(a) (b)

Figure 13: Continued.

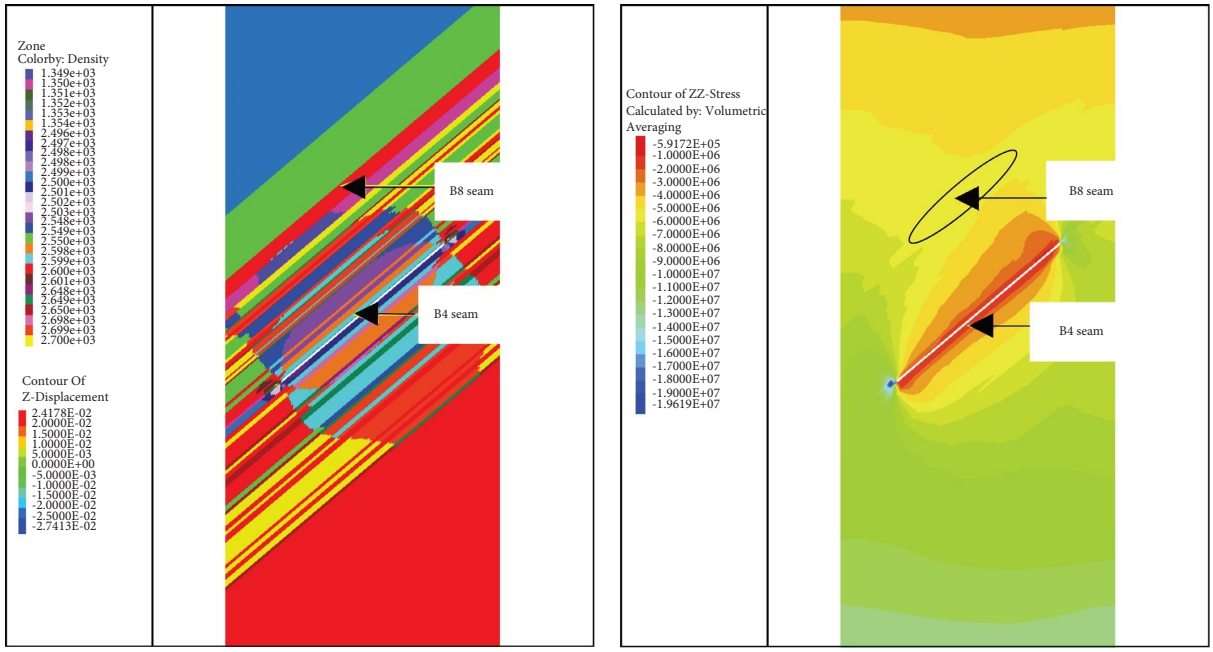

(c) (d)

Figure 13: Cloud map of the influence of B4 coal seam mining on B8 coal seam: cloud map of (a) plastic zone distribution, (b) vertical displacement distribution, (c) density variation distribution, and (d) vertical stress distribution.

is 700 m, the width is 250 m, the height is 322 m, and the excavation length of the working face is 114 m. The specific model is shown in Figure 14.

First of all, on the basis of the initial model, the working face is excavated 100 m, and the return air roadway of the adjacent lower face is tunneled 100 m. At this point, the distance between the mining face and the heading face is 400 m, and the equilibrium is calculated. After mining 40 m in each working face, the distance between the two sides is shortened by 40 m until the mining face tunnels the heading face; that is, the distance between the two sides is −120 m. The influence of two-sided disturbance is simulated, and some of the results are shown in Figure 15.

As shown in Figure 15, when the mining distance of the working face is 100 m and 180 m, the maximum pressure around the working face is 11 MPa and 13.5 MPa, respectively, which is located on the side of the transport roadway. At this point, the maximum pressure of the return air roadway of the adjacent working face is 6 MPa, and the two sides do not disturb each other. When the mining face is 300 m, the maximum pressure around the working face is 16.3 MPa, which is located on the side of the two roadways. The pressure in front of the working face is less than that of the two roadways, and the maximum value is 11.2 MPa. At this point, the maximum pressure of the return air roadway in the adjacent working face is 6.2 MPa, and there is some disturbance on the two sides. When the mining face is 540 m, the pressure around the working face obviously affects the return air roadway of the adjacent working face.

In order to further reveal the influence of working face mining on the adjacent return air roadway, the numerical simulation results are extracted. When the working face is advanced at different distances, the maximum pressure around the working face and on the return air roadway is shown in Figure 16.

It can be observed from Figure 16 that the maximum pressure around the working face and above the return air roadway has gone through three stages with an increase in the mining distance of the working face. The first stage is when the mining distance of the working face is less than 260 m. In this stage, the maximum pressure around the working face increases linearly with an increase in the mining distance and the maximum pressure above the return air roadway remains unchanged, so there is no disturbance on both sides. The second stage is when the mining distance of the working face is more than 300 m and less than 500 m. In this stage, the maximum pressure around the working face increases gradually with an increase in the mining distance and the increasing speed gradually slows down; the maximum pressure above the return air roadway increases gradually with an increase in the mining distance but does not increase significantly, so there is a slight disturbance on both sides. The third stage is when the mining distance of the working face is more than 500 m. In this stage, the maximum pressure around the working face changes only slightly with an increase in the mining distance, and the maximum pressure above the return air roadway increases sharply with an increase in the mining distance and gradually approaches the maximum pressure around the mining face, so there is serious disturbance on both sides. According to the results shown in Figure 16, when the distance between the working face and the return air roadway gradually shortens during the advancing process of the working face, the interaction between the two gradually

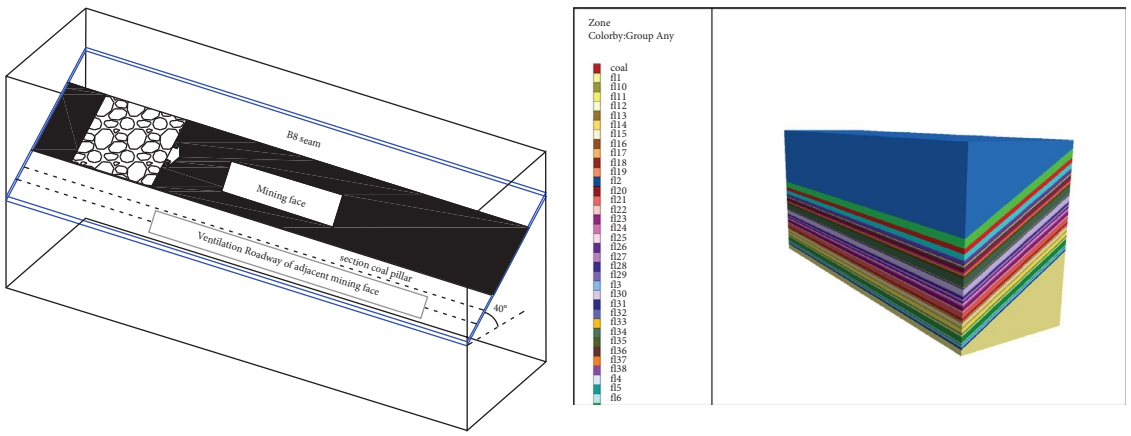

(a) (b)

Figure 14: Model diagram of the working face and numerical simulation: (a) model diagram of the working face; (b) numerical model diagram of the working face.

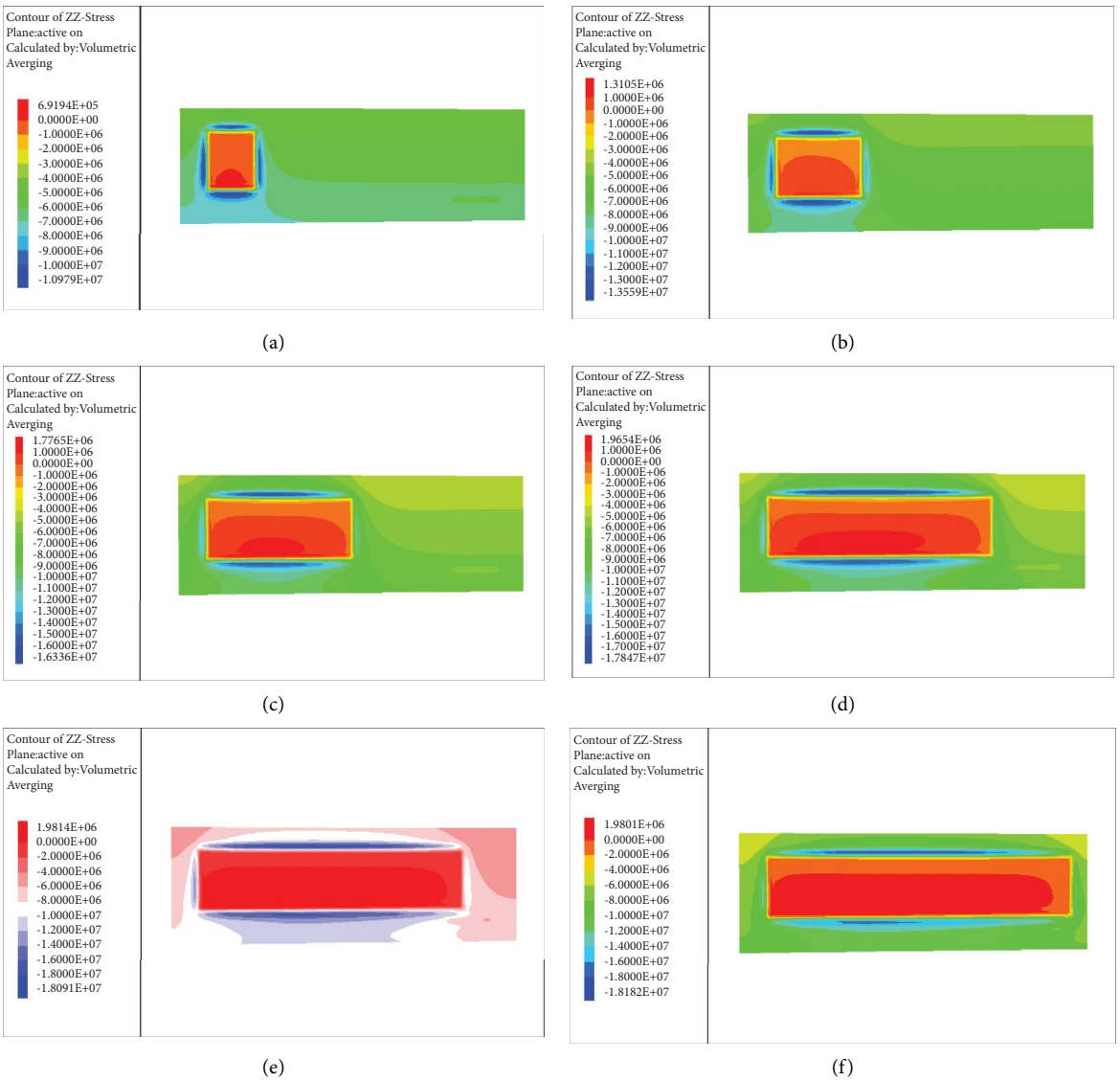

(a) (b)

(c) (d)

(e) (f)

Figure 15: Cloud map of vertical stress distribution at different mining distances in the working face: (a) working face mining 100 m; (b) working face mining 180 m; (c) working face mining 300 m; (d) working face mining 460 m; (e) working face mining 540 m; (f) working face mining 620 m.

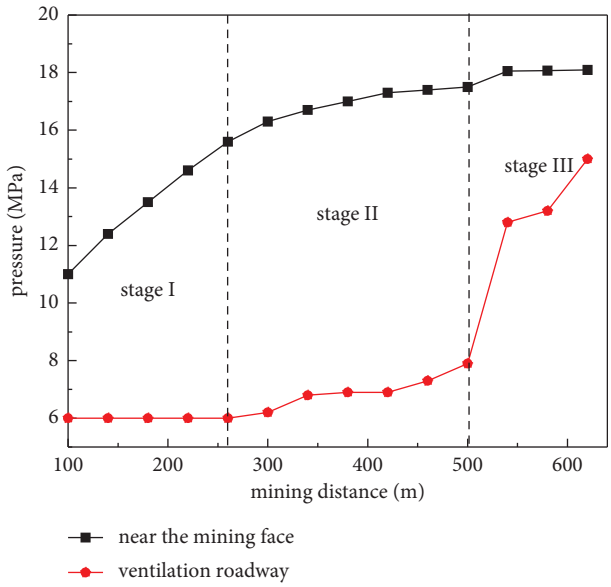

Figure 16: Variation of the maximum pressure of the working face and return air roadway with the mining distance of the working face.

increases. At this time, the pressure above the working face and the roadway gradually increases, which may cause a series of safety problems. Therefore, measures such as accelerating the advancing speed of the working face, shortening the roof overhang time, and reducing the top control distance of the working face can be actively taken to reduce the concentration of the abutment pressure. At the same time, when the distance between the working face and the return air roadway is within the range of the third stage, reasonable support measures should be taken.

It is worth noting that the numerical simulation results are obtained according to the specific geological and mining conditions of Xiaogou coal mine. Based on the above analysis, the mining pressure behavior law of the working face, the coal pillar with different widths, and interaction between coal seams in the Xiaogou coal mine mining process are obtained. At the same time, the influence of coal seam mining on the adjacent air return roadway is analyzed. The specific numerical results of the above analysis are only applicable to Xiaogou coal mine, however, the above simulation and theoretical analysis methods can be applied to the mining of large dip coal seams under different geological conditions.

4. Conclusions

Taking the B8 coal seam of Xiaogou coal mine in Nanshan coal mine as the research object, this paper explores the law of pressure behavior in the mining process of steeply inclined coal seams. Through the methods of the theoretical analysis and numerical simulation, this paper delves into the pressure behavior law of the coal pillar above and the section of the mining face in a high-dip coal seam, as well as the interaction between steeply inclined coal seams and the pressure behavior during the interaction between the mining face and adjacent return air roadway. The main conclusions are as follows:

(1) The range of the plastic zone of the inclined abutment pressure of the working face is related to the dip angle of the coal seam, which is not noticeable when the dip angle of the coal seam is small, but with an increase in the dip angle of the coal seam, the difference in the plastic zone of the abutment pressure between the upper side and the lower side of the coal pillar increases. During the mining of the steeply inclined coal seams, the stress concentration in the lower part of the working face deviates to the roof and the stress concentration in the upper face deviates to the floor, which is obviously different from that in the gently inclined coal seams.

(2) The vertical stress above the coal pillar in the section changes in three stages with an increase in the width of the coal pillar: In the first stage, the overall bearing pressure of the coal pillar is larger and is on one side of the roadway when the width of the coal pillar is small. In the second stage, with an increase in the width of the coal pillar, the peak stress is far from the roadway and the influence of the roof of the goaf on the roadway begins to decrease. In the third stage, when the width of the roadway coal pillar continues to increase, the stress on the side of the coal pillar is no longer superimposed on each other. Therefore, based on the numerical simulation results and the recovery rate, this paper proposes a reasonable solution of leaving section coal pillars; that is, the coal pillar width of the second stage is taken as the section coal pillar width. Through the numerical simulation and theoretical analysis, the reasonable width of the section coal pillar is analyzed quantitatively, and the results are consistent, which show the reliability and stability of this method. When mining the working face of large inclined seams on-site, corresponding pressure relief measures should be taken at the lower roof and upper floor of the working face to reduce the effect of the abutment pressure.

(3) In the process of mining steeply inclined coal seams, the maximum pressure around the working face and above the return air roadway goes through three stages with an increase in the mining distance of the working face: the stage of no mutual influence, the stage of slight mutual influence stage, and stage of serious mutual influence. When the distance between the working face and the return air roadway is within the range of the third stage during the field mining of large dip coal seams, measures such as speeding up the advancing speed of the working face, shortening the roof extension time, and reducing the control distance of the top of the working face should be taken to reduce the top surface pressure concentration. At the same time, reasonable support measures shall be taken.

Data Availability

The data can be obtained from the corresponding author on request.

Conflicts of Interest

The authors declare that they have no conflicts of interest.

Acknowledgments

This study was supported by the National Science Foundation for Young Scientists of China (Grant no. 52004170).

References

[1] J. Zhang, J. Wang, W. Weijie, C. Yi, and Z. Song, "Experimental and numerical investigation on coal drawing from thick steep seam with longwall top coal caving mining," *Arabian Journal of Geosciences*, vol. 11, no. 5, pp. 1–19, 2018.

[2] Y. Wu, H. Jingyu, P. Xie, B. Hu, and K. Liu, "Mechanism of instability of section coal pillar in steeply dipping seam based on large-scale strata control technology," *Journal of China Coal Society*, vol. 43, no. 11, pp. 3062–3071, 2018.

[3] W. Yang, B. Lin, Y. Qu et al., "Mechanism of strata deformation under protective seam and its application for relieved methane control," *International Journal of Coal Geology*, vol. 85, no. 3-4, pp. 300–306, 2011.

[4] C. Y. Liu, J. X. Yang, and F. F. Wu, "A proposed method of coal pillar design, goaf filling, and grouting of steeply inclined coal seams under water-filled strata," *Mine Water and the Environment*, vol. 34, no. 1, pp. 87–94, 2015.

[5] S. L. Zaĭtsev, "Physiological evaluation of the work of facemen and crew of the combine brigade in the Donbass mines with steeply sloping coal seams," *Gigiena Truda i Professionalnye Zabolevaniia*, vol. 15, no. 3, pp. 24–27, 1971.

[6] F. Ren, X. Lai, and M. Cai, "Dynamic destabilization analysis based on AE experiment of deep-seated, steep-inclined and extra-thick coal seam," *Journal of University of Science and Technology Beijing, Mineral, Metallurgy, Material*, vol. 15, no. 3, pp. 215–219, 2008.

[7] D. Deb, C. Sunwoo, and Y. Jung, "Pit optimization for steep coal seams at Pasir coal mine, Indonesia," *Journal of the Korean Society of Mineral and Energy Resources Engineers*, vol. 46, no. 5, pp. 509–520, 2009.

[8] X. Qi, R. Wang, and W. Mi, "Failure characteristics and control technology of surrounding rock in deep coal seam roadway with large dip angle under the influence of weak structural plane," *Advances in Civil Engineering*, vol. 2020, Article ID 6623159, 17 pages, 2020.

[9] H. Tu, S. Tu, D. Zhu, D. Hao, and K. Miao, "Force-fracture characteristics of the roof above goaf in a steep coal seam: a case study of xintie coal mine," *Geofluids*, vol. 2019, Article ID 7639159, 11 pages, 2019.

[10] P. Yang and C. Liu, "Failure law and control technology of surrounding rock in fully mechanized mining gateway of steep seam," *Disaster Advances*, vol. 6, pp. 172–181, 2013.

[11] T. Hong-Sheng, T. Shi-Hao, Z. Cun, Z. Lei, and Z. Xiao-Gang, "Characteristics of the roof behaviors and mine pressure manifestations during the mining of steep coal seam," *Archives of Mining Sciences*, vol. 62, no. 4, pp. 871–891, 2017.

[12] J. Wu, H. Jing, Y. Gao, Q. Meng, Q. Yin, and Y. Du, "Effects of carbon nanotube dosage and aggregate size distribution on mechanical property and microstructure of cemented rock-fill," *Cement and Concrete Composites*, vol. 127, Article ID 104408, 2022.

[13] C. Xue, A. Cao, G. Wenhao et al., "Energy evolution law and rock burst mechanism of deep thick seams with large inclination," *Journal of Mining and Safety Engineering*, vol. 38, no. 5, pp. 876–885, 2021.

[14] W. B. Lu, Y. Wu, J. Chen, and H. Fu, "Safety analysis of tunnel in gob of high steep thick coal seam (I)-2-D numerical simulation for response," *Applied Mechanics and Materials*, vol. 71–78, pp. 1532–1538, 2011.

[15] J. Zhang and W. Shi, "Deformation and failure features of surrounding rock for combining mining in steep and close seam," *Applied Mechanics and Materials*, vol. 327, pp. 338–341, 2013.

[16] H. Zhang, L. Xu, M. Yang, C. Deng, and Y. Cheng, "Pressure relief mechanism and gas extraction method during the mining of the steep and extra-thick coal seam: a case study in the yaojie No. 3 coal mine," *Energies*, vol. 15, no. 10, pp. 3792–3817, 2022.

[17] Y. Wu, P. Xie, and S. Ren, "Analysis of spatial asymmetric structure characteristics of surrounding rock in large dip seam mining," *Journal of Coal Industry*, vol. 35, no. 2, pp. 182–184, 2010.

[18] G. Xie, K. Yang, and Q. Liu, "Study on distribution laws of stress in inclined coal pillar for fully-mechanized top-coal caving face," *Chinese Journal of Rock Mechanics and Engineering*, vol. 25, no. 3, pp. 545–549, 2006.

[19] J. Xie and J. Xu, "Effect of key stratum on the mining abutment pressure of a coal seam," *Geosciences Journal*, vol. 21, no. 2, pp. 267–276, 2017.

[20] J. Cao, "Study on reasonable size of coal pillars in large dip angle coal seam," in *Proceedings of the 2019 International Conference on Environmental Protection*, pp. 71–74, Coal Industry and Metallurgical Mine Safety, Rome, Italy, April 2019.